Earth and Planetary Science Letters 448 (2016) 94–101

Contents lists available at ScienceDirect

Earth and Planetary Science Letters

www.elsevier.com/locate/epsl

Global seismic data reveal little water in the mantle transition zone

C. Houser

Earth-Life Science Institute, Tokyo Institute of Technology, 2-12-1-IE-1 Ookayama, Meguro-ku, Tokyo, 152-8550, Japan

ARTICLE INFO

Article history:
Received 7 January 2016
Received in revised form 15 March 2016
Accepted 19 April 2016
Available online 27 May 2016
Editor: B. Buffett

Keywords:
mantle transition zone
mantle discontinuities
mantle shear velocity
SS precursors
mantle phase transitions

ABSTRACT

Knowledge of the Earth's present water content is necessary to constrain the amount of water and other volatiles the Earth acquired during its formation and the amount that is cycled back into the interior from the surface. This study compares 410 and 660 km discontinuity depth with shear wave tomography within the mantle transition zone to identify regions with seismic signals consistent with water. The depth of the 410 and 660 km discontinuities is determined from a large updated dataset of SS-S410S and SS-S660S differential travel times, known as SS precursors. The discontinuity depths measured from binning and stacking the SS precursor data are then compared to the shear velocity model HMSL-S06 in the transition zone. Mapping all the possible combinations, very few locations match the predictions from mineral physics for the effects of water on discontinuity depth and shear velocity. The predictions, although not yet measured at actual transition zone temperatures and pressures, are a shallow 410 km discontinuity, a deep 660 km discontinuity, and a slow shear velocity. Only 8% of the bins with high-quality data are consistent with these predictions, and the calculated average water content within these bins is around 0.6 wt.%. A few isolated locations have patterns of velocity/topography that are consistent with water, while there are large regional-scale patterns consistent with cold/hot temperature anomalies. Combining this global analysis of long period seismic data and the current mineral physics predictions for water in transition zone minerals, I find that the mantle transition zone is generally dry, containing less than one Earth ocean of water. Although subduction zones could be locally hydrated, the combined discontinuity and velocity data show no evidence that wadsleyite or ringwoodite have been globally hydrated by subduction or initial Earth conditions.

1. Introduction

Understanding the Earth's water budget through time requires constraining the amount of water that is currently present in the Earth's interior. The amount of water in the interior could be decreasing over time by degassing at divergent plate boundaries, increasing by transport within subducting oceanic plates, or in balance between these processes. Water may be able to reach the mantle transition zone within metastable mineral phases in cold subducting oceanic lithosphere (i.e. slabs) (Angel et al., 2001). Mineral physics studies have shown that nominally anhydrous wadsleyite and ringwoodite could contain close to 3% water (Inoue et al., 1995; Kohlstedt et al., 1996), which is a storage capacity of up to 10 oceans of water. Since planetary formation models are sensitive to the Earth's initial water content, it is necessary to put bounds on the amount of water in this potential reservoir. The mantle transition zone is here defined by global seismic reflectors consistent with phase transitions in the olivine component of the mantle at approximately 410 km (olivine to wadsleyite) and 660 km depth (ringwoodite to bridgmanite and ferropericlase).

Several studies have measured the effects of water on the properties of transition zone minerals and will be summarized briefly here. While wadsleyite and ringwoodite can hold up 3 wt.% water at ambient conditions (Smyth et al., 2004; Ohtani et al., 2000), the capacity for water storage decreases with increasing temperature such that 1–2 wt.% is often predicted at transition zone temperatures and pressures (Bolfan-Casanova et al., 2006; Mao et al., 2008), but could be as low as 0.2 wt.% (Dixon et al., 2002; Huang et al., 2005; Hirschmann, 2006; Inoue et al., 2010; Mao et al., 2012). Inoue et al. (2004) found that the seismologically observed bulk sound speed contrast across 410 km discontinuity is consistent with a bulk composition that is 60% olivine and 1.5 wt.% water. They also measured a lower density and bulk sound velocity for hydrous compared to anhydrous wadsleyite. Ab initio calculations indicate that both shear and compressional velocity will decrease by 1.5% for each 1.0 wt.% water added to hydrous wadsleyite (up to the maximum of 3.3 wt.%) (Tsuchiya and Tsuchiya, 2009). Smyth and Frost (2002) observed that water will stabilize wadsleyite relative to olivine, and therefore decrease the depth

E-mail address: chouser@elsi.jp.

http://dx.doi.org/10.1016/j.epsl.2016.04.018
0012-821X/

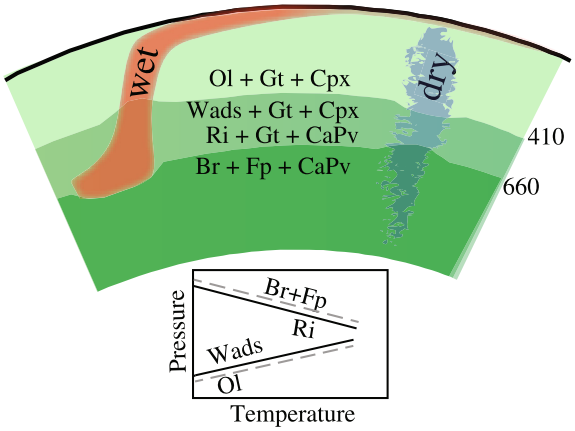

Fig. 1. Cartoon representing the predicted behavior (see Jacobsen and Smyth, 2006) of transition zone phases in the presence of a downwelling wet slab or dry mantle upwelling colored red/blue because water reduces shear velocity (ignoring temperature). The schematic phase diagram shows the Clapeyron slopes of dry (black solid) and wet (gray dashed) olivine component of the mantle. Ol = olivine, Gt = garnet, Cpx = clinopyroxene, Wads = wadsleyite, Ri = ringwoodite, CaPv = calcium perovskite, Br = bridgmanite, and Fp = ferropericlase. (For interpretation of the references to color in this figure legend, the reader is referred to the web version of this article.)

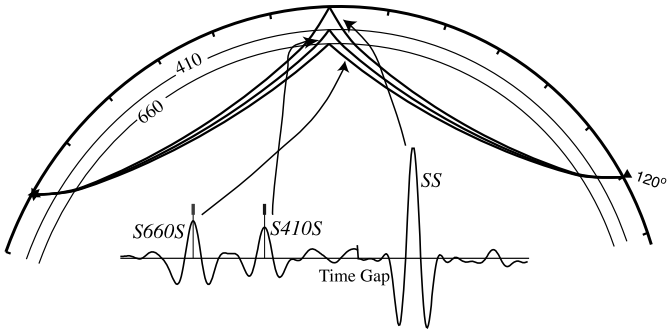

Fig. 2. Ray geometry of *SS* precursors, and an actual precursor stack used in this study from the NW Pacific including 1133 seismograms. There is a time gap between the main *SS* arrival and the precursors. The vertical lines at the pulse peak are the SdS arrival times and the small gray lines above the pulse represent the error in the pulse peak from the bootstrap random resampling.

Table 1
SS precursor arrival time measurements.

Author	Start	End	Number of data
Flanagan and Shearer (1998)	1976	1995	13,467
Houser et al. (2008a)	1995	2005	26,348
Update	2006	2010	31,577
Total for this study	1976	2010	71,392

of the transition such that the 410 km discontinuity would be shallower (lower pressure) in the presence of water. By the same reasoning, since water is more compatible in ringwoodite than bridgmanite and ferropericlase, the 660 km discontinuity is deeper (higher pressure) for a hydrous peridotite composition (Litasov et al., 2005). In addition to these experimental results, Pearson et al. (2014) measured 1.4 wt.% water in a ringwoodite inclusion in a natural diamond.

Thio et al. (2016) point out that there have been no experiments that measure properties of transition zone materials at both the high temperatures and pressures for water-bearing phases. From a thermodynamic point of view, since water is more easily incorporated into wadsleyite than olivine at the top of the transition zone and ringwoodite than bridgmanite and ferropericlase at the base of the transition zone, water will expand the stability fields of wadsleyite and ringwoodite and increase the thickness of the transition zone. This scenario could change if other minerals that can incorporate water become stable at the high temperatures and pressures of the transition zone. However, the consensus from mineral physics (Jacobsen and Smyth, 2006; Bolfan-Casanova et al., 2006) is that the seismic signature of 1–2 wt.% water present in the mantle transition zone is slow shear velocity, shallow 410 km discontinuity, and deep 660 km discontinuity, Fig. 1.

Mineral physics predictions can be tested by comparing global maps of shear wave velocity and discontinuity depth (Helffrich, 2002). Despite the fact that global tomographic models have decreased resolution in the mantle transition zone, most tomographic models are in generally good agreement about the large scale features such as the emergence of subducted slabs (Ritsema et al., 2004). Global maps of discontinuity topography are constructed by measuring the time difference between the surface-reflected SS phase and the S410S and S660S reflections (see Fig. 2 and further discussion in the methods section). Although they use different methods, there are several reliable global discontinuity studies from SS precursors which are also in relatively good agreement about the large scale features (Deuss, 2009). Thus, general conclusions can be made by combining any tomography and discontinuity model to examine which regions may be compatible with the presence of water. Here I compare an updated map of discontinuity topography to the shear velocity model HMSL-S06 (Houser et al., 2008b).

2. Method

I use the same data and methodology as (Houser et al., 2008a) to obtain the SS-S410S and SS-S66SS differential times from 2006 to 2010. Since the S410S and S660S arrivals are too faint to be seen above the noise on most individual seismograms, I stack seismograms with high quality SS signals whose bounce points lie within 5° radius bins (Fig. 2). The traces are first deconvolved by the main SS pulse and then aligned and stacked according to their arrival times measured using cluster analysis (Houser et al., 2008b). The SS-S410S and SS-S660S differential times are converted to depth using 20 s PREM (Dziewonski and Anderson, 1981). For a full description of the stacking procedure, see Houser et al. (2008a).

This update increases the amount of measured SS arrival times by over 40% (Table 1) and improves the SS precursor stack quality in the northern Pacific, southern Pacific, eastern Asia, Indian ocean, northern South America, and north Atlantic. Fig. 3 shows the increase in the number of traces per stack in each bin and representative stacks from the many different regions before and after the update. While the improvement in coverage is dominant in the Pacific and eastern Asia, there is improvement in a variety of tectonic settings. The resulting maps of topography on the 410 and 660 km discontinuity and transition zone thickness are shown in Fig. 4. I used the total combined dataset from Flanagan and Shearer (1998), Houser et al. (2008a), and the updated dataset of 2006–2010 for the SS precursor stacking. While the update improves coverage in several regions, there are still many areas in the southern hemisphere that have too few data to obtain a quality stack. In Figs. 4, 6 and 7, I do not plot areas where the depth error exceeds 20 km.

I compare the updated discontinuity topography to a shear velocity model with the same inversion method as HMSL-S06 but parameterized with 6° equal-area blocks (Fig. 5). I use the 530–660 km depth layer within the transition zone parameterized at 6° (not 4° as in the original HMSL-S06; Houser et al., 2008b) to be consistent with the broader sensitivity of the SS precursors. The upper mantle is constrained by surface wave phase velocity maps